



OPEN ACCESS

EDITED BY

Yan Huang,
Anhui Medical University, China

REVIEWED BY

Rong Pan,
Stony Brook University, United States
Charles Elias Assmann,
Federal University of Santa Maria, Brazil

*CORRESPONDENCE

Xifan Mei,
✉ meixifan@jzmu.edu.cn
He Tian,
✉ tianhe@jzmu.edu.cn
Zhaoliang Shen,
✉ szl13274163111@163.com

†These authors have contributed equally to this work

RECEIVED 12 October 2024

ACCEPTED 10 January 2025

PUBLISHED 29 January 2025

CITATION

Li D, Bai M, Guo Z, Cui Y, Mei X, Tian H and Shen Z (2025) Zinc regulates microglial polarization and inflammation through IKB α after spinal cord injury and promotes neuronal repair and motor function recovery in mice. *Front. Pharmacol.* 16:1510372. doi: 10.3389/fphar.2025.1510372

COPYRIGHT

© 2025 Li, Bai, Guo, Cui, Mei, Tian and Shen. This is an open-access article distributed under the terms of the [Creative Commons Attribution License \(CC BY\)](https://creativecommons.org/licenses/by/4.0/). The use, distribution or reproduction in other forums is permitted, provided the original author(s) and the copyright owner(s) are credited and that the original publication in this journal is cited, in accordance with accepted academic practice. No use, distribution or reproduction is permitted which does not comply with these terms.

Zinc regulates microglial polarization and inflammation through IKB α after spinal cord injury and promotes neuronal repair and motor function recovery in mice

Daoyong Li^{1,2†}, Mingyu Bai^{1,2†}, Zhanpeng Guo², Yang Cui^{1,2}, Xifan Mei^{1,2*}, He Tian^{2,3*} and Zhaoliang Shen^{1*}

¹The Third Affiliated Hospital of Jinzhou Medical University, Jinzhou City, Liaoning, China, ²Key Laboratory of Liaoning Medical Organization Engineering, Jinzhou, Liaoning, China, ³School of Basic Medicine, Jinzhou Medical University, Jinzhou, Liaoning, China

Introduction: Spinal cord injury (SCI) leads to severe inflammation and neuronal damage, resulting in permanent loss of motor and sensory functions. Zinc ions have shown potential in modulating inflammation and cellular survival, making them a promising therapeutic approach for SCI. This study investigates the mechanisms of zinc ion treatment in SCI, focusing on its effects on inflammation.

Methods: We used transcriptomic analysis to identify key pathways and genes involved in the inflammatory response in a mouse model of SCI. *In vitro* studies assessed the impact of zinc ions on inflammation, cell polarization, and apoptosis. IKB α expression was evaluated as a potential target of zinc ions, both in cultured cells and *in vivo*.

Results: Transcriptomic analysis revealed that zinc ions modulate inflammatory pathways through IKB α , which inhibits NF- κ B activity. *In vitro*, zinc treatment upregulated IKB α expression, reducing inflammation, polarization, and apoptosis. These results were confirmed in the SCI mouse model, where zinc ions also reduced inflammation and cell death.

Discussion: Our findings highlight a novel mechanism by which zinc ions regulate inflammation in SCI by upregulating IKB α and inhibiting NF- κ B activation. This suggests potential therapeutic applications of zinc ions in SCI and other inflammatory conditions, warranting further investigation into their clinical benefits.

KEYWORDS

spinal cord injury, zinc, microglial polarization, inflammatory response, functional recovery

Abbreviations: SCI, Spinal cord injury; TNF, α tumor necrosis factor- α ; IL, 1 β interleukin-1 β ; IL, 6 interleukin-6; NF, κ B nuclear factor κ B.

1 Introduction

SCI is a catastrophic neurological disorder characterized by direct physical damage to the spinal cord and a subsequent complex cascade of secondary injuries (Huang et al., 2022). These secondary responses, including inflammation, oxidative stress, apoptosis, and glial scar formation, exacerbate the already compromised neural tissue, leading to further loss of neurological function (Pajarillo et al., 2022). SCI patients often face long-term disability, with severe motor and sensory impairments significantly affecting their quality of life and social participation (Iaffaldano et al., 2021).

Inflammatory responses play a central role in the pathophysiology of SCI. Following mechanical injury to the spinal cord, an initial primary injury is immediately triggered, after which inflammatory responses are rapidly activated, becoming a major driver of secondary damage (Brennan et al., 2022). This process involves multiple cellular and molecular mechanisms, where microglia at the injury site and peripherally infiltrating macrophages rapidly adopt a pro-inflammatory phenotype, releasing copious amounts of inflammatory mediators such as tumor necrosis factor- α (TNF- α), interleukin-1 β (IL-1 β), and interleukin-6 (IL-6) (Fan et al., 2020; Van Broeckhoven et al., 2022). These mediators not only exacerbate the local inflammatory environment but also activate downstream signaling pathways, such as nuclear factor κ B (NF- κ B) and mitogen-activated protein kinase pathways, further amplifying the inflammatory response (Muñoz García et al., 2024). Additionally, inflammatory mediators induce a cascade of cytokine reactions, leading to the recruitment of more immune cells to the injury site, creating a vicious cycle that persistently aggravates neural tissue damage (Groeger et al., 2010). Therefore, inflammatory responses present both challenges and opportunities in the neuroprotection and repair processes following SCI. A thorough understanding and effective regulation of these responses are crucial for mitigating the long-term impact of SCI.

Microglia are the primary immune cells in the central nervous system, and they swiftly activate and exhibit different polarization states following SCI, primarily classified into M1 and M2 types (Caffarel and Braza, 2022; Mizobuchi and Soma, 2021). M1 microglia are pro-inflammatory, secreting large amounts of inflammatory mediators such as TNF- α , IL-1 β , and nitric oxide, which exacerbate neuronal damage and death, thereby expanding the injury zone (Zhao et al., 2020). In contrast, M2 microglia possess anti-inflammatory and reparative properties, secreting anti-inflammatory factors like IL-10 and TGF- β , promoting neuroprotection and tissue repair (Tan et al., 2019). However, the post-SCI environment typically favors M1 polarization, leading to sustained inflammation and neuronal damage. Therefore, regulating microglial polarization to promote a shift towards the M2 phenotype is a crucial strategy for reducing inflammation and facilitating neural repair (Liu et al., 2020; Sun et al., 2022).

Zinc ions, as a crucial trace element, perform various biological functions in the nervous system, including neurotransmitter release, synaptic plasticity, neuroprotection, and injury repair. Dysregulation of zinc homeostasis is linked to the pathophysiology of neurodegenerative diseases such as

Alzheimer's, Parkinson's, and ischemic stroke (Mo et al., 2022). Zinc promotes SCI recovery by accelerating neuronal autophagy and inhibiting apoptosis, and it regulates NLRP3 inflammasome activity via autophagy and ubiquitination. Additionally, zinc alleviates neuronal apoptosis by modulating mitochondrial quality control post-SCI (Jiang et al., 2023; Li et al., 2020).

Based on this background, our study aims to investigate whether zinc ions can modulate the inflammatory response of microglia by regulating key inflammatory genes, and whether this modulation impacts neuroprotection and motor function recovery post-SCI. This research will elucidate the mechanisms of zinc ions in SCI treatment, providing a scientific basis for developing new therapeutic strategies and ultimately improving the quality of life for SCI patients.

2 Materials and methods

2.1 Cell culture and treatment

Mouse BV2 microglia and PC12 neuron cell lines were purchased from the cell bank of the Chinese Academy of Sciences. They were cultured in Dulbecco's modified Eagle's medium (DMEM, Hyclone, UT, United States) supplemented with 10% fetal bovine serum (FBS, Gibco, CA, United States), 100 units/mL penicillin and 100 μ g/mL streptomycin (Gibco, Grand Island, NY, United States). All cells were cultured in a humidified incubator containing 5% CO₂ and 95% air at 37°C, and the cell culture medium was changed every 2 days. After the cell state is stabilized, the LPS (0.5 μ g/mL) and BV2 cells were incubated for 24 h to induce the cells to be in a state of inflammatory damage, and then used in each group of experiments. Then, Zinc Gluconate (ZnG) (100 μ Mol) was incubated with the treated BV2 cells for 24 h. Then, the cell tissues of each group were collected for subsequent experiments.

2.2 Cell viability

BV2 cells were seeded in 96-well plates (5,000 cells/well) and incubated at 37°C with 5% CO₂ for 24 h. Different doses of Zinc were then added to different wells and the cells were incubated for another 24 h. Finally, 20 μ L CCK-8 (Btyotime, China) solution and 180 μ L fresh medium were added to each well, and incubated together at 37°C for 1 h, and the absorbance measured at 450 nm using a microplate reader (Synergy-2, BioTek, Winooski, VT, United States).

2.3 Cell transfection

To silence NF-kappa-B inhibitor alpha (IKBa), si-IKBa (genefarma, Shanghai, China) was transfected into BV2 cells in the presence of Lipofectamine 3,000 reagent (Thermo Scientific, United States) according to the manufacturer's protocol. At the same time, a negative control (NC) was used for simultaneous transfection. Use Western blotting (WB) to confirm transfection efficiency. IKBa siRNA, sense: 5'-CCAUGAAGGACGAGGAGU

TABLE 1 Primers used for qRT-PCR.

Gene	Forward	Reverse
IKBa	GCTGGAAGGCAGAAAGTGAAGG	TGCAGGCTCTATCGGGTATTT
MAP2	GACAGAGAAACAGCAGAGGAAGTG	TGTTCTGATGCTGGCGATGGT
IL-1 β	GTTGACGGACCCAAAAGAT	AAGGTCCACGGGAAAAGACAC
IL-6	TAGTCCTTCTACCCCAATTTCC	TTGGTCCTTAGCCACTCCTTC
CD206	AGTGATGGTTCTCCTGTTTCC	GGTGTAGGCTCGGGTAGTAGT
CD68	ACGTATTGGAAGGAGATTACAGCT	TCTGTCAGCGTTACTATCCCGC
Arg-1	GAACACGGCAGTGGCTTTAAC	TGCTTAGCTCTGCTGCTTTGC
GAPDH	CAAGTTCAACGGCACAGTCAAG	ACATACTCAGCACCAGCATCAC
RPS18	AGGATGTGAAGGATGGGAAG	TTCTTCAGCCTCTCCAGGTC

ATT-3'; anti-sense:5'-UACUCCUCGUCCUUAUGGTT-3'. NC siRNA, sense: 5'-UUCUCCGAACGUGUCACGUTT -3'; anti-sense: 5'-ACGUGACACGUUCGGAGA ATT -3'.

2.4 Quantitative real-time PCR

Total RNA was extracted using Trizol (Qiagen, Hilden, Germany) from BV2 cells, PC12 cells, or 1.5 cm long spinal cord tissue centered at the site of spinal cord injury, according to the manufacturer's protocol (Sang et al., 2024). RNA was then quantified using the NanoDrop 1,000 spectrophotometer (Thermo Scientific, United States), followed by reverse transcription using the Superscript[®] III reverse transcription Kit (Invitrogen, Waltham, Ma, United States). Quantitative real-time PCR (qRT-PCR) was performed using the Quantifast SYBR[®] green PCR kit (Qiagen, Hilden, Germany) on the Applied Biosystems 7500HT Fast Real-Time PCR System. Murine ribosomal protein S18 (RPS18) was then amplified on all samples as a housekeeping gene and internal control to explain changes in mRNA levels. Finally, the $(1 + e)^{-\Delta\Delta CT}$ method was used to compare the target gene in the experimental group with the corresponding target gene in the control group. All primer sequences used in this experiment are shown in Table 1.

2.5 Neuron-microglia cocultures

As shown in Figure 6A, Transwell establishes a PC12 cell-BV2 cell system that is independent of contact, as described previously. Briefly, PC12 cells (8×10^5 /well) were first seeded in 6-well plates and treated with LPS (0.5 μ g/mL) for 24 h. At the same time, the BV2 cells (4×10^5 /well) inoculated in the inserts of each group were incubated together for 24 h under different treatment factors. Then, the insert washed with PBS was directly added above the PC12 cells, and the culture was continued in a 6-well plate. The 2 cells were cultured together for 12 h, sharing the same medium. After the end of co-cultivation, neurotoxicity was analyzed using lactate dehydrogenase (LDH) release and qPCR on MAP2 gene expression.

2.6 Determination of LDH content

After the PC12 cells in each group were treated with different reagent combinations, the activity of LDH was measured using a test kit (Jiancheng Bioengineering Research Institute, China) according to the manufacturer's protocol. The absorbance was then measured at 450 μ m using a Varioskan Flash Reader (Thermo Scientific, Waltham, MA, United States).

2.7 Animals

According to previous studies (Xu et al., 2023), animal experiments were conducted in C57BL/6 mice (20–35 g, 10–12 weeks) each half of females and males. All mice were purchased from Beijing Vital River Laboratory Animal Technology Co., Limited in Beijing, China. All operative procedures were approved by the animal experimental ethics committee of Jinzhou Medical University. All animals were kept under controlled conditions in a 12 h light/dark cycle at 23°C, with food and water available *ad libitum*.

2.8 SCI model and animal grouping

The model of contusion spinal cord injury in mice was established using the modified weight-drop method. Mice were intraperitoneally injected with ketamine (75 mg/kg) and xylazine (3 mg/kg) for anesthesia. The hair centered on T9 was cut and the skin disinfected, then the skin was cut, the muscle tissue separated, and the spinal cord exposed. An impactor with a diameter of 2 mm and a weight of 12.5 g was used to strike the surface of the spinal cord from a height of 5 cm at T9, causing moderate contusion. Mice in a sham operation group underwent laminectomy but were not struck with an impactor. The wounds were then closed and the mice returned to the cage. They were helped to urinate twice a day until the voluntary urination function was restored. For the experimental procedure, the mice were categorized into four distinct groups: Sham (Laminectomy Only), SCI (Spinal Cord Injury), Zinc (Intraperitoneal ZnG (30 mg/kg) injection 2 h post-spinal

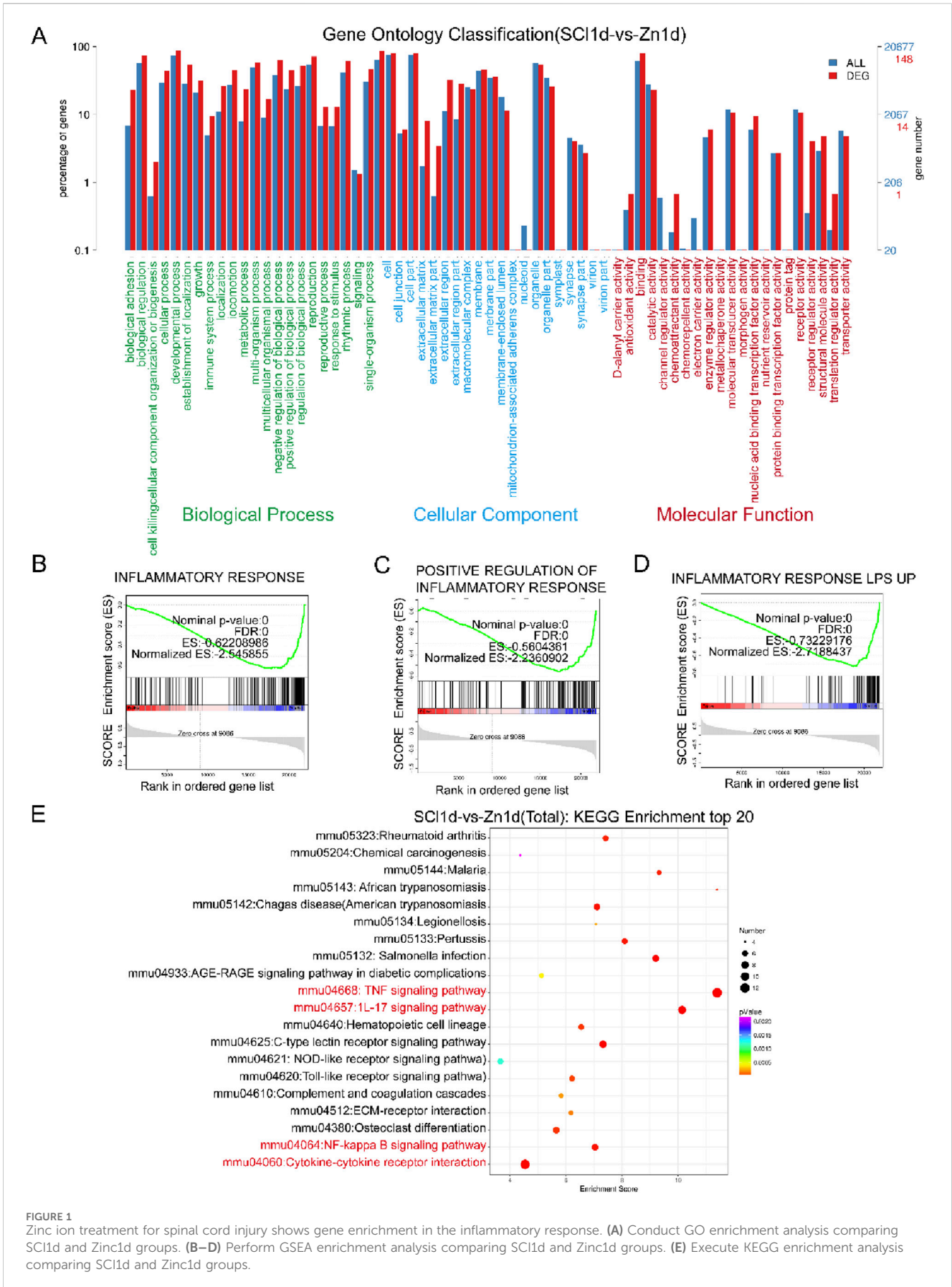


FIGURE 1 Zinc ion treatment for spinal cord injury shows gene enrichment in the inflammatory response. (A) Conduct GO enrichment analysis comparing SCI1d and Zinc1d groups. (B–D) Perform GSEA enrichment analysis comparing SCI1d and Zinc1d groups. (E) Execute KEGG enrichment analysis comparing SCI1d and Zinc1d groups.

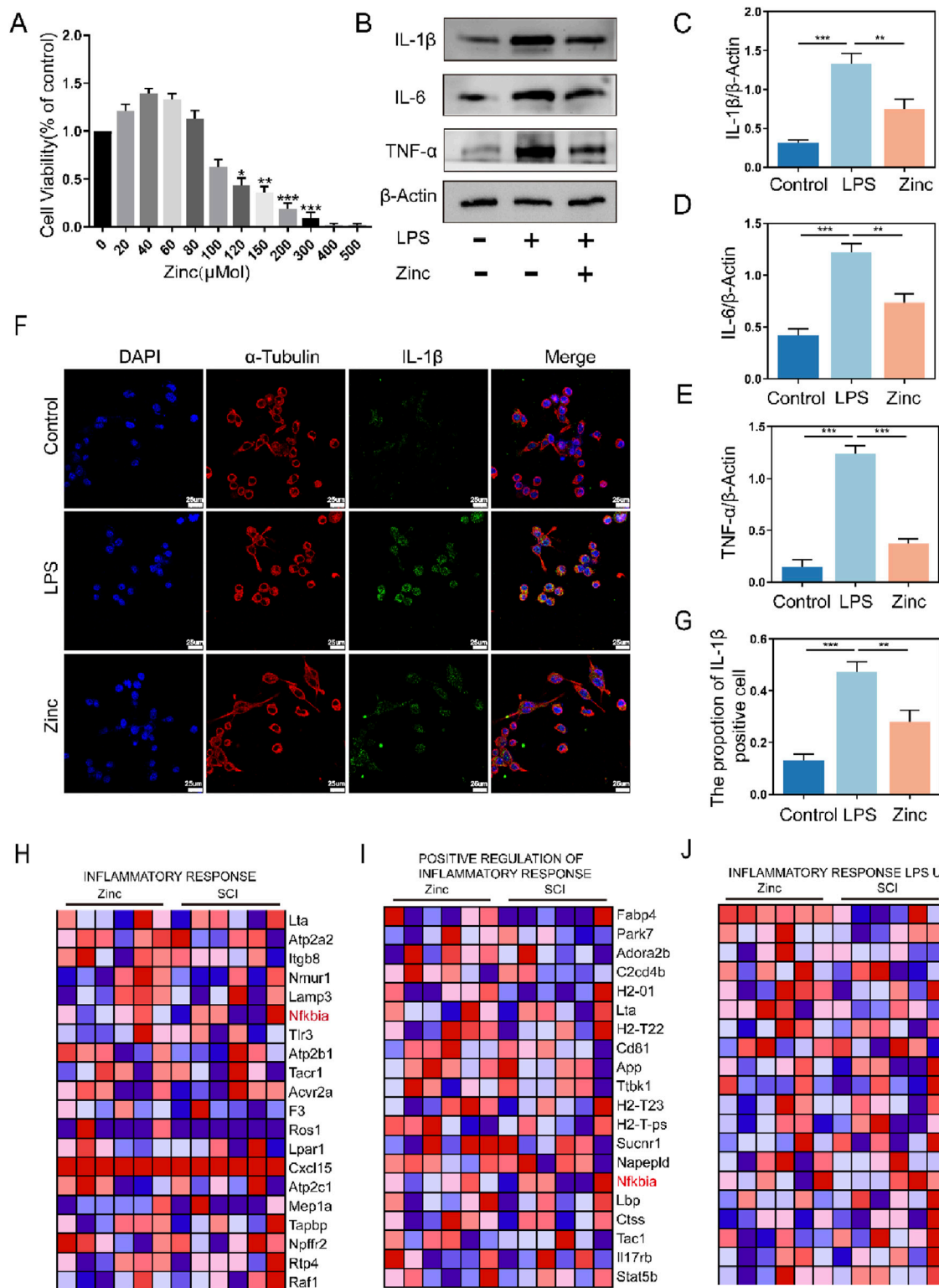


FIGURE 2 Zinc ions inhibit the expression of inflammatory cytokines in BV2 cells. **(A)** Assessment of BV2 cell viability under varying concentrations of Zinc (μMol). **(B–E)** Representative Western blot images and quantifications of IL-1β, IL6, and TNF-α in BV2 cells from Control, LPS (0.5 μg/mL), and Zinc (100 μMol) groups, n = 6. **(F, G)** Representative immunofluorescence images and quantifications of IL-1β in BV2 cells from Control, LPS, and Zinc groups, scale bar = 25 μm, n = 6. **(H–J)** Core genes identified through GSEA enrichment analysis comparing SCI1d and Zinc1d groups. Data presented the mean ± SD, *p < 0.05, **p < 0.01, and ***p < 0.001.

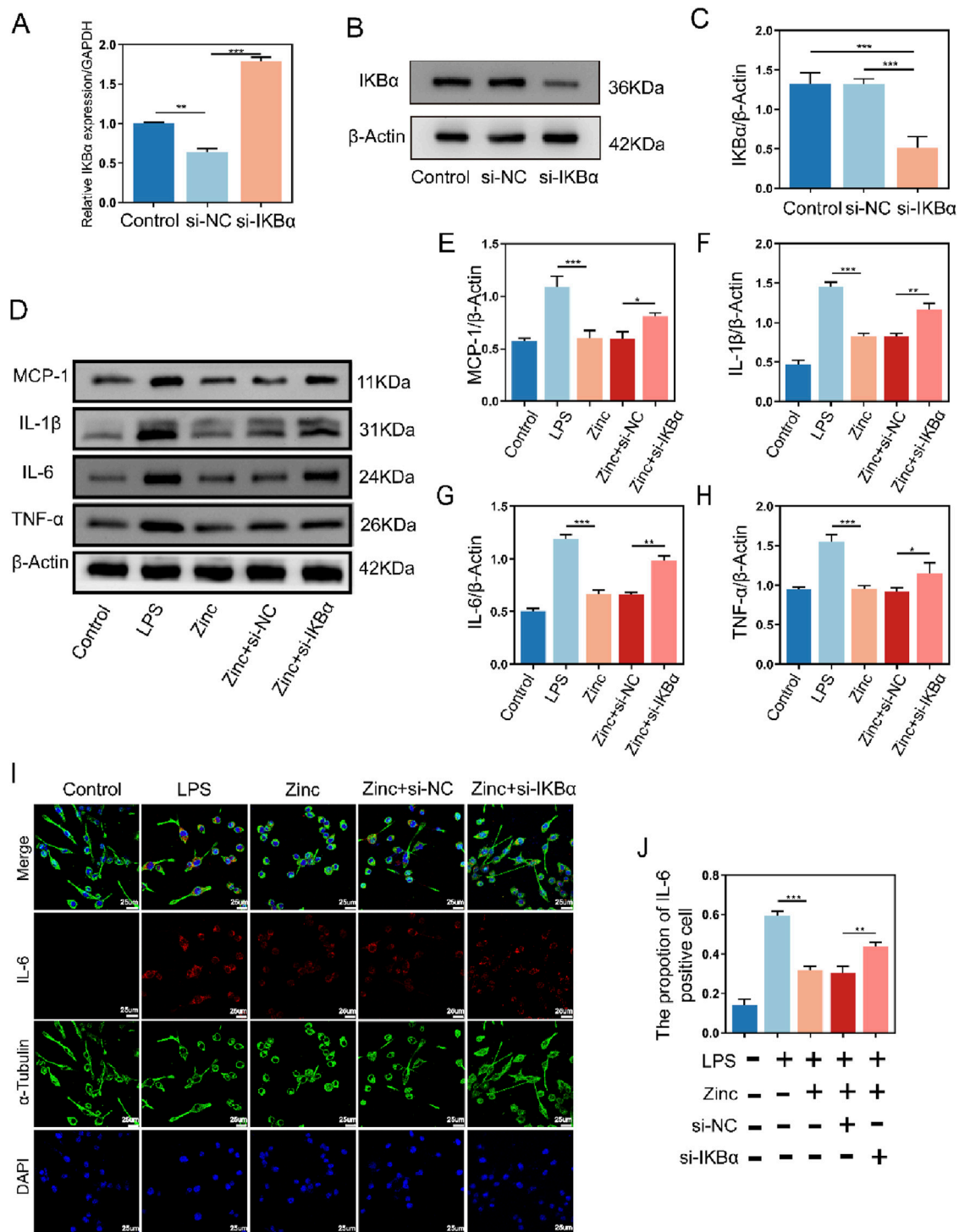


FIGURE 3
 Zinc ions elevate IκBα to suppress inflammatory cytokine expression in BV2 cells. (A) Quantitative PCR analysis of IκBα expression in BV2 cells from Control, si-NC, and si-IκBα groups. (B, C) Representative Western blot images and quantifications of IκBα expression in BV2 cells from Control, si-NC, and si-IκBα groups, n = 6. (D–H) Representative Western blot images and quantifications of MCP1, IL-1β, IL6, and TNF-α expression in BV2 cells from Control, LPS (0.5 μg/mL), Zinc (100 μMol), Zinc + si-NC, and Zinc + si-IκBα groups, n = 6. (I, J) Representative immunofluorescence images and quantifications of IL6 in BV2 cells from Control, LPS (0.5 μg/mL), Zinc (100 μMol), Zinc + si-NC, and Zinc + si-IκBα groups, scale bar = 25 μm, n = 6. Data presented the mean ± SD, *p < 0.05, **p < 0.01, and ***p < 0.001.

cord injury surgery, 1 time/d until day 3.) and BAY 11–7,082 (Intraperitoneal ZnG (30 mg/kg) and injection 2 h post-spinal cord injury surgery, 1 time/d until day 3. And 10 μg/day BAY

11–7,082, injection 2 h post-spinal cord injury surgery, 1 time/d until day 3.)The timing and dose of ZnG and BAY 11–7,082 were based on previous studies (Deng et al., 2023).

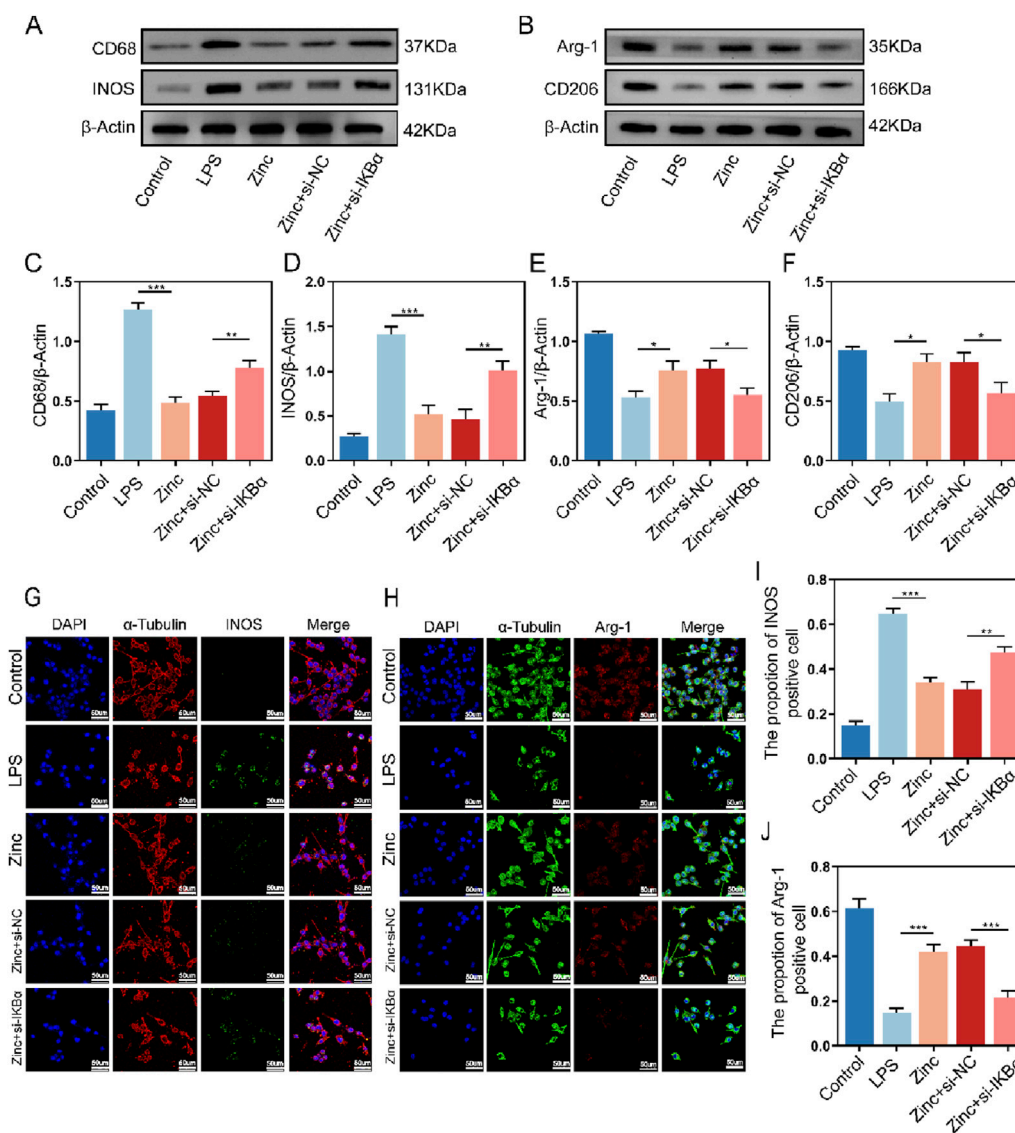


FIGURE 4 Zinc ions elevate IkBa to promote M2 polarization while reducing M1 polarization in BV2 cells. (A, C, D) Representative Western blot images and quantifications of CD68 and INOS expression in BV2 cells from Control, LPS (0.5 μg/mL), Zinc, Zinc + si-NC, and Zinc + si-IkBa groups, n = 6. (B, E, F) Representative Western blot images and quantifications of CD206 and Arg-1 expression in BV2 cells from Control, LPS (0.5 μg/mL), Zinc (100 μMol), Zinc + si-NC, and Zinc + si-IkBa groups, n = 6. (G–J) Representative immunofluorescence images and quantifications of INOS and Arg-1 in BV2 cells from Control, LPS, (0.5 μg/mL) Zinc, Zinc + si-NC, and Zinc + si-IkBa groups, scale bar = 50 μm, n = 6. Data presented the mean ± SD, *p < 0.05, **p < 0.01, and ***p < 0.001.

2.9 Western blot analysis

BV2 cells were collected after 24 h of drug treatment. Mouse spinal cord tissue was collected on the third day after injury for protein analysis, and Western blotting was performed following Methods detailed in (Irrera et al., 2017). The main antibodies and concentration used in this experiment are as follows: anti-IL-1β (1:1,000, abcam, Cambridge, United Kingdom); anti-IL-6 (1:1,000, abcam, Cambridge, United Kingdom); anti-TNF-α (1:1,000, abcam, Cambridge, United Kingdom); anti-β-Actin (1:10,000, abcam, Cambridge, United Kingdom); anti-IkBa (1:1,000, abcam, Cambridge, United Kingdom); anti-CD68 (1:1,000, abcam, Cambridge, United Kingdom); anti-INOS (1:1,000, Cell Signaling

Technology, Inc., Danvers, MA, United States); anti-Arg1 (1:1,000, abcam, Cambridge, United Kingdom); anti-CD206 (1:1,000, Cell Signaling Technology, Inc., Danvers, MA, United States); anti-MCP1 (1:500, abcam, Cambridge, United Kingdom). Finally, enhanced chemiluminescence reagents (Thermo Fisher Scientific) were used to visualize the results and ImageJ software (NIH, Bethesda, MD, United States) was used to analyze the density of protein bands.

2.10 Immunofluorescence analysis

Spinal cord slices from each experimental group were removed from storage at -80°C and rewarmed at room temperature for 2 h,

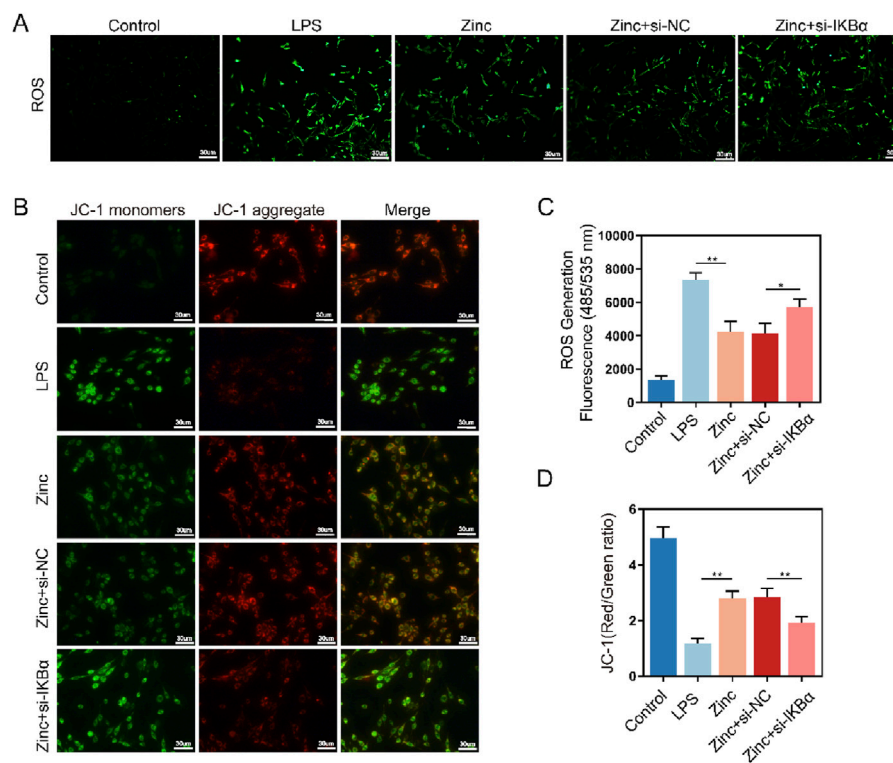


FIGURE 5
Zinc ions elevate IκBα to inhibit oxidative stress in BV2 cells. (A, C) Representative ROS fluorescence probe images and quantifications in BV2 cells from Control, LPS (0.5 μg/mL), Zinc (100 μMol), Zinc + si-NC, and Zinc + si-IκBα groups, scale bar = 20 μm, n = 6. (B, D) Representative JC-1 fluorescence probe images and quantifications in BV2 cells from Control, LPS (0.5 μg/mL), Zinc, Zinc + si-NC, and Zinc + si-IκBα groups, scale bar = 30 μm, n = 6. Data presented the mean ± SD, *p < 0.05, **p < 0.01, and ***p < 0.001.

and the cells from each experimental group were fixed with 4% paraformaldehyde in a cell culture dish. The slices and cells were then separately incubated with 0.3% tritonx-100 for 15 min and with goat serum for 2 h. Primary antibodies were then incubated with spinal cord slices and cells separately overnight in a 4°C humidified chamber. The main antibodies and concentration are as follows: anti-IL-1β (1:500 abcam, Cambridge, United Kingdom); anti-INO (1:500 abcam, Cambridge, United Kingdom); anti-IL-6 (1:500 abcam, Cambridge, United Kingdom); anti-Arg-1 (1:500 abcam, Cambridge, United Kingdom); anti-Anti-β-III Tubulin (1:500, abcam, Cambridge, United Kingdom); anti-Iba-1 (1:1,000, abcam, Cambridge, United Kingdom); anti-α-Tubulin (1:1,000, abcam, Cambridge, United Kingdom); anti-GFAP (1:500, abcam, Cambridge, United Kingdom). The primary antibody was then eluted with PBS and the spinal cord tissue and cells were incubated with Alexa fluor 488 Goat anti rabbit IgG or Alexa fluor 594 Goat anti mouse IgG (1:250, Thermo Fisher Science) for 2 h at room temperature. The spinal cord tissue and cells were washed three times with PBS for 5 minutes and the nuclei stained with 40,6-diaminodinitro-2-benzoindeole solution (DAPI) (Invitrogen, Carlsbad, CA, United States) for 20 min. Finally, results were observed under a fluorescence microscope (Olympus Hamburg, Germany), and the optical density of fluorescence was analyzed using ImageJ2x software.

2.11 TUNEL staining

TUNEL staining was performed on the spinal cord sections one days after SCI with an in situ apoptosis detection kit (Jiancheng Institute of Bioengineering, Nanjing, China). Spinal cord slices from each experimental group were rewarmed at room temperature for 2 h and then washed three times with PBS for 5 min each time. The washed spinal cord sections were cultured with 0.3% Triton X-100 at 4°C for 15 min and then washed again three times with PBS and incubated with TUNEL reaction mixture in a dark, humid environment at 37°C for 60 min. They were then washed again three times with PBS for 3 min each time, and incubated with DAPI for 10–15 min. Finally, the spinal cord sections were observed and photographed under a microscope.

2.12 Measurements of mitochondrial ROS

Mitochondrial ROS levels were quantified using MitoSOX™ Red fluorescent dye (M36008, Invitrogen) according to the manufacturer's instructions. Cells were incubated in MitoSOX™ Red-containing medium for 30 min, washed, and then analyzed by flow cytometry. Data were analyzed using FlowJo v10.8.1 software.

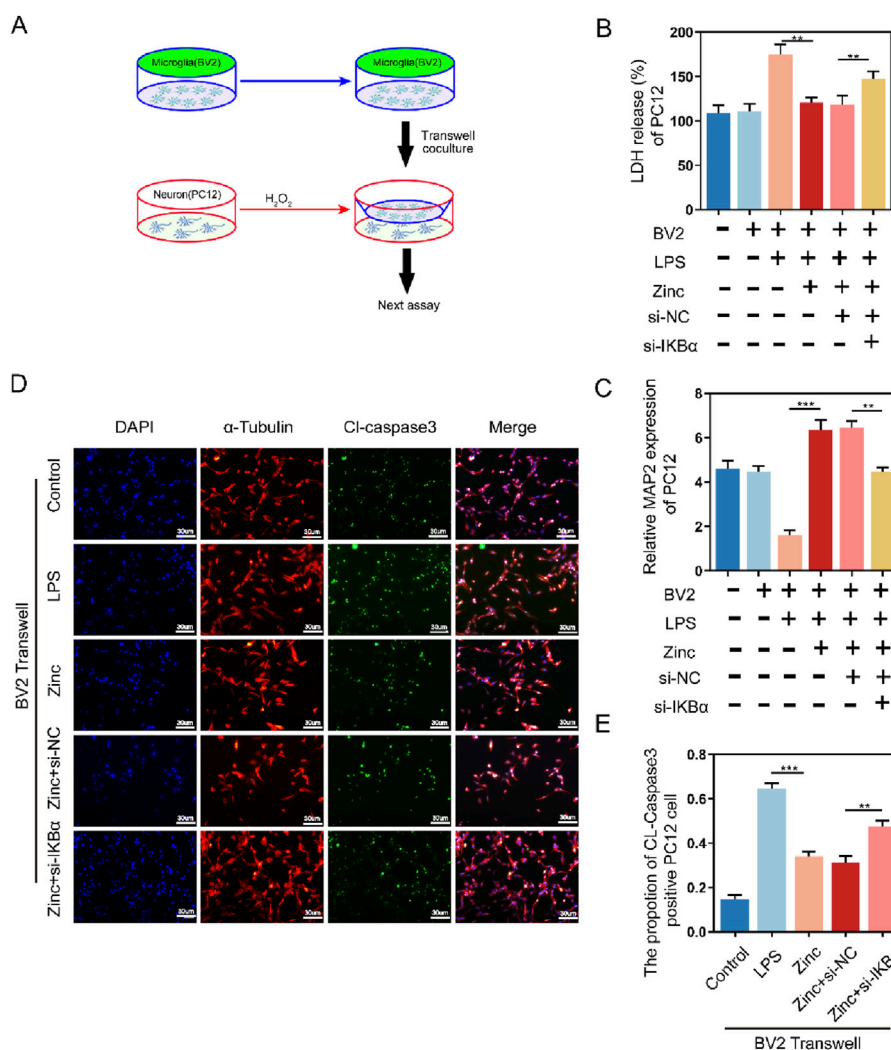


FIGURE 6 Zinc ions elevate IκBα to inhibit the pro-apoptotic effect of BV2 cells on PC12 cells. (A) Schematic illustration of Transwell assay with BV2 and PC12 cells. (B) LDH activity and quantifications in PC12 cells following Transwell exposure to Control, LPS (0.5 μg/mL), Zinc (100 μMol), Zinc + si-NC, and Zinc + si-IKβα groups, n = 6. (C) MAP-2 expression and quantifications in PC12 cells following Transwell exposure to Control, LPS (0.5 μg/mL), Zinc (100 μMol), Zinc + si-NC, and Zinc + si-IKβα groups, n = 6. (D, E) Representative immunofluorescence images and quantifications of CL-Caspase3 in PC12 cells following Transwell exposure to Control, LPS (0.5 μg/mL), Zinc (100 μMol), Zinc + si-NC, and Zinc + si-IKβα groups, scale bar = 30 μm, n = 6. Data presented the mean ± SD, *p < 0.05, **p < 0.01, and ***p < 0.001.

2.13 Mitochondrial membrane potential assay (ΔψM)

Mitochondrial membrane potential was assessed using a JC-1 Mitochondrial Membrane Potential Assay Kit (Beyotime, China). Cells were stained with 2.0 μg/mL JC-1 dye at 37°C for 20 min, washed, and examined under a fluorescence microscope. The analysis involved the relative fluorescence ratio technique, comparing the red/green fluorescence ratios of apoptotic, necrotic, and viable cells. In healthy cells, JC-1 accumulates in the mitochondrial matrix, emitting red fluorescence, while a decrease in membrane potential results in monomeric JC-1 and green fluorescence. To maintain objectivity, an independent researcher captured five random images per group using a Leica DMi8 fluorescence microscope (Wetzlar, Germany). Fluorescence intensity per pixel was quantified using ImageJ

software, with uniform threshold adjustments, and the average pixel intensity was calculated to represent the mean fluorescence intensity for each group.

2.14 Statistical analysis

SPSS statistical software (Chicago, Illinois, United States) was used for analysis. All data were expressed as mean ± standard deviation (SD). Shapiro-Wilk test was used to evaluate the data distribution. The two groups were analyzed by Mann-Whitney U test. When there were more than two groups, we used one-way ANOVA, Bonferroni's post test (when the variances were equal) and Kruskal-Wallis test (when the variances were not equal) to compare multiple groups. BMS score was analyzed using a two-way ANOVA

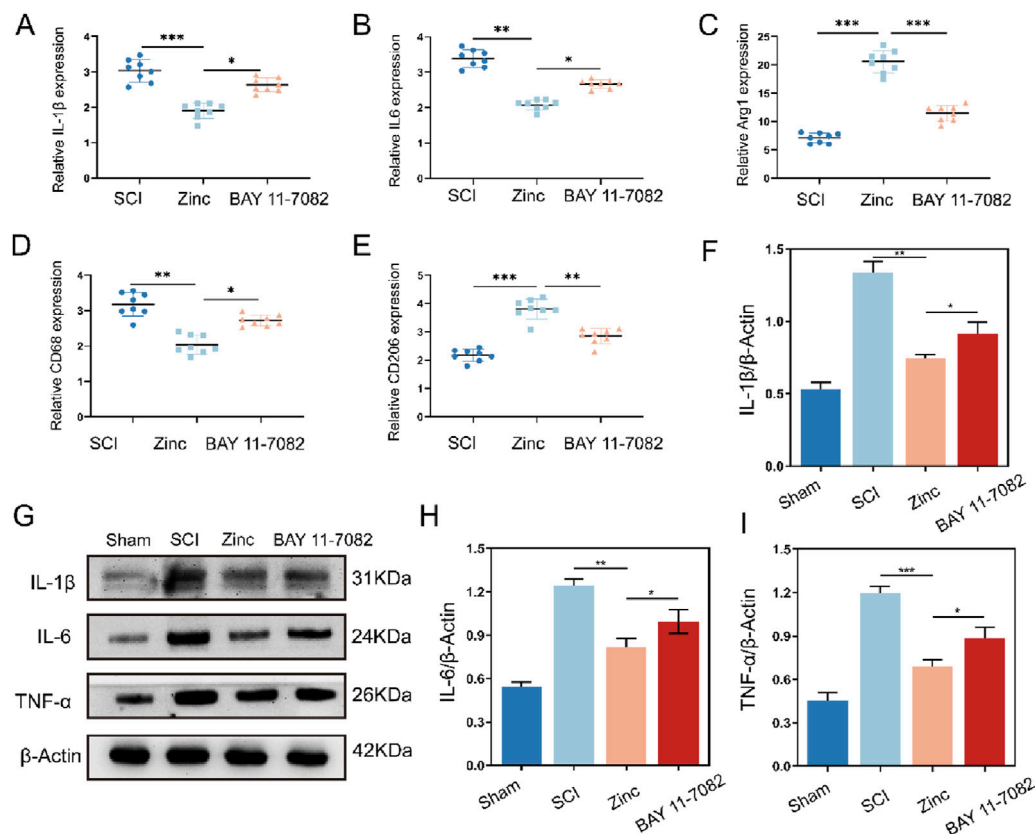


FIGURE 7

Zinc ions elevate I κ B α to inhibit cytokine expression and M1 polarization of microglia in mice with spinal cord injury. (A–E) Quantitative PCR analysis of IL-1 β , IL-6, Arg1, CD68, and CD206 in spinal cord tissues from SCI, Zinc (30 mg/kg), and BAY11-7,082 groups of mice, $n = 8$. (F–I) Representative Western blot images and quantifications of IL-1 β , IL-6, and TNF α in spinal cord tissues from SCI, Zinc, and BAY11-7,082 groups of mice, $n = 6$. Data presented the mean \pm SD, * $p < 0.05$, ** $p < 0.01$, and *** $p < 0.001$.

with Tukey's *post hoc* test. For all tests, Significance levels were defined as $p < 0.05$ (*), $p < 0.01$ (**), $p < 0.001$ (***)

3 Results

3.1 Zinc ion treatment for spinal cord injury shows gene enrichment in the inflammatory response

One day post-SCI, upon zinc ion treatment, our GO enrichment analysis revealed that compared to the injured group, the zinc-treated group exhibited enriched biological processes related to factor regulation and signaling, indicating increased signaling protein transmission (Figure 1A). Subsequent GSEA enrichment analysis showed a significant number of genes enriched in gene sets associated with inflammatory response, positive regulation of the inflammatory response, and LPS-induced inflammation, highlighting the critical regulatory role of zinc ions in the inflammatory response of SCI mice (Figures 1B–D). Furthermore, our KEGG enrichment analysis identified changes in inflammatory pathways such as TNF signaling and NF- κ B signaling (Figure 1E). These findings underscore the paramount importance of zinc ion's regulatory effects on inflammation in SCI treatment.

3.2 Zinc ions inhibit the expression of inflammatory cytokines in BV2 cells

To validate the anti-inflammatory effects of zinc ions *in vitro*, we first determined the optimal concentration for zinc ions on cell viability (Figure 2A). Using Western blot analysis, we assessed the expression of inflammatory cytokines IL-1 β , IL-6, and TNF- α , and found that zinc ions significantly inhibited their expression (Figures 2B–E). In the LPS-stimulated BV2 cell model, zinc ions effectively suppressed IL-1 β expression (Figures 2F, G). After preliminarily confirming the anti-inflammatory effects of zinc ions, we further screened core genes from the GSEA-enriched gene sets and identified NFKBia as a pivotal gene consistently involved in inflammation clusters. As a transcriptional gene for I κ B α , we hypothesize that zinc ions may alleviate inflammation post-SCI by promoting I κ B α production.

3.3 Zinc ions elevate I κ B α to suppress inflammatory cytokine expression in BV2 cells

To verify whether the increase in I κ B α is crucial for the anti-inflammatory effects of zinc ions, we transfected BV2 cells to inhibit I κ B α expression and confirmed the transfection efficiency (Figures

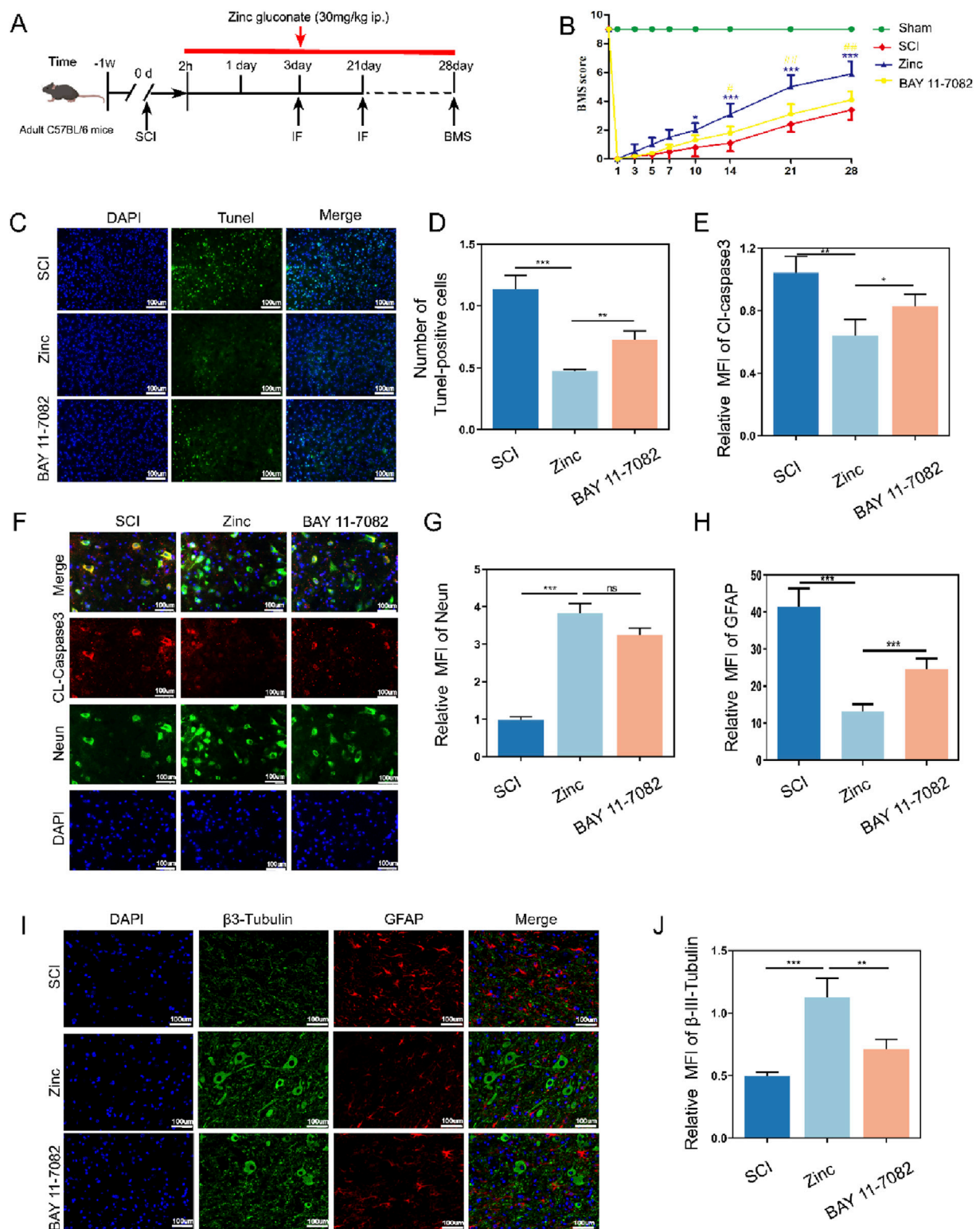


FIGURE 8 Zinc ions elevate IxBa, enhancing motor function, reducing neuronal apoptosis, and limiting glial scar formation in mice with spinal cord injury. **(A)** Schematic diagram of post-spinal cord injury detection in mice. **(B)** BMS scores in mice from SCI, Zinc, and BAY11-7082 groups. **(C, D)** Representative TUNEL staining images and quantifications of spinal cord tissues from SCI, Zinc (30 mg/kg), and BAY11-7082 groups, scale bar = 100 μm, n = 6. **(E–G)** Representative immunofluorescence images and quantifications of CL-Caspase3 and Neun in spinal cord tissues from SCI, Zinc, and BAY11-7082 groups, scale bar = 100 μm, n = 6. **(H–J)** Representative immunofluorescence images and quantifications of GFAP and βIII-Tubulin in spinal cord tissues from SCI, Zinc, and BAY11-7082 groups, scale bar = 100 μm, n = 6. Data presented the mean ± SD, *p < 0.05, **p < 0.01, and ***p < 0.001.

3A–C). Using Western blot analysis, we assessed the expression of MCP-1, IL-1 β , IL-6, and TNF- α . Compared to the Zinc group, which showed inhibition of inflammatory cytokines, the Zinc + si-IK β A group lost this inhibitory effect, and the expression of inflammatory proteins increased. This indicates that the original inhibitory effect of zinc ions on inflammatory cytokine expression is counteracted by the inhibition of IK β A (Figures 3D–H). Cell fluorescence analysis of IL-6 confirmed the Western blot results, demonstrating that the increase in IK β A is closely related to the anti-inflammatory effects of zinc ions (Figures 3I, J).

3.4 Zinc ions elevate I κ B α to promote M2 polarization while reducing M1 polarization in BV2 cells

Microglia, as the crucial inflammatory cells in the central nervous system, have their polarization states closely tied to inflammatory responses. Through Western blot analysis, we found that under LPS stimulation, microglia exhibit increased expression of CD68 and iNOS, indicating M1 polarization, which is associated with pro-inflammatory responses. Conversely, the expression of CD206 and Arg-1, markers of M2 microglia linked to anti-inflammatory effects, decreased. Zinc ion treatment shifted microglia towards the anti-inflammatory M2 polarization. However, when IK β A was knocked down, the ability of zinc ions to modulate microglial polarization was inhibited, causing microglia to re-polarize towards the pro-inflammatory M1 state (Figures 4A–F). Further cell fluorescence analysis confirmed that zinc ions promote microglial M2 polarization through upregulation of IK β A (Figures 4G–J).

3.5 Zinc ions elevate I κ B α to inhibit oxidative stress in BV2 cells

Microglial inflammatory responses and polarization are closely linked to mitochondrial homeostasis. To further investigate the effect of zinc ions on mitochondria in microglia, we used ROS probes to detect intracellular ROS generation. Zinc ions significantly reduced ROS production; however, this inhibitory effect was abolished with the knockdown of IK β A (Figures 5A, C). Subsequently, using the JC-1 assay kit, we assessed mitochondrial membrane potential stability. We found that zinc ions depend on increased IK β A expression to maintain mitochondria predominantly in an aggregated state, thereby stabilizing the mitochondrial membrane potential (Figures 5B, D). Our experiments further confirmed the critical role of IK β A in zinc ion-mediated maintenance of intracellular homeostasis.

3.6 Zinc ions elevate I κ B α to inhibit the pro-apoptotic effect of BV2 cells on PC12 cells

Microglia are also crucial for neuronal survival. To further explore the interaction between microglia and neurons, we used a Transwell system, culturing BV2 cells in the upper chamber and

PC12 cells in the lower chamber (Figure 6A). Zinc-treated BV2 cells significantly enhanced the survival of PC12 cells, as evidenced by the LDH assay showing increased PC12 cell survival. Additionally, MAP2 expression analysis in PC12 cells revealed that zinc-treated PC12 cells exhibited more mature neuronal phenotypes. However, these protective effects of zinc ions were diminished when IK β A was knocked down in BV2 cells (Figures 6B, C). Cell fluorescence imaging further demonstrated that zinc-treated BV2 cells reduced CL-Caspase3 expression in PC12 cells, an effect that was inhibited with the knockdown of IK β A in BV2 cells (Figures 6D, E).

3.7 Zinc ions elevate I κ B α to inhibit cytokine expression and M1 polarization of microglia in mice with spinal cord injury

In vitro experiments demonstrated that zinc ions play a positive role in reducing the expression of inflammatory factors, regulating microglial polarization, and protecting neurons, with these effects being closely associated with increased intracellular IK β A. To comprehensively validate our findings, we conducted further experiments in a mouse model of spinal cord injury. Using PCR, we measured the expression of IL-1 β , IL-6, CD68, CD206, and Arg1 in the injured spinal cords. Zinc ions suppressed the transcription of pro-inflammatory cytokines and markers while enhancing the transcription of anti-inflammatory markers. However, these effects were blocked when the mice were treated with the IK β A inhibitor BAY 11–7,082 (Figures 7A–E). Western blot analysis confirmed these results at the protein level (Figures 7F–I). Additionally, tissue fluorescence analysis showed that zinc ions inhibited M1 polarization and promoted M2 polarization of IBA1-positive microglia in the injured spinal cords, an effect reversed by BAY 11–7,082 (Supplementary Figures 1A–D). These findings corroborate our in vitro results, indicating that zinc ions modulate microglial inflammation and polarization by upregulating IK β A.

3.8 Zinc ions elevate I κ B α , enhancing motor function, reducing neuronal apoptosis, and limiting glial scar formation in mice with spinal cord injury

Finally, we investigated the recovery of mice after zinc ion treatment (Figure 8A). Mice treated with zinc ions showed a gradual improvement in motor function scores (Figure 8B). TUNEL staining and CL-Caspase3 tissue fluorescence staining indicated that zinc ion treatment provided significant anti-apoptotic effects in spinal cord injury models (Figures 8C–G). Additionally, long-term tissue analysis revealed that zinc ions inhibited glial scar formation, as shown by reduced GFAP and β III-Tubulin expression, an effect dependent on increased IK β A expression (Figures 8H–J). In summary, our in vivo studies confirm that zinc ions promote motor function recovery and reduce glial scar formation after spinal cord injury, with these effects being dependent on the upregulation of IK β A.

4 Discussion

In this study, we explored the potential mechanisms and therapeutic effects of zinc ions in the treatment of spinal cord injury (SCI). Through transcriptomic analysis, we revealed that zinc ions mitigate the pathological processes of SCI by modulating the inflammatory response (Ge et al., 2021). Our findings suggest that the anti-inflammatory effects of zinc ions may be mediated by upregulating I κ B α expression. As a key regulator of inflammation, I κ B α was shown in vitro to reduce the production of inflammatory factors, influence microglial polarization, and inhibit apoptosis in PC12 cells, with these effects being dependent on increased I κ B α expression. Our in vivo experiments in a mouse model of spinal cord injury further confirmed these conclusions, supporting that zinc ions exert their anti-inflammatory effects and promote motor function recovery by upregulating I κ B α .

SCI is a severe neurological condition characterized by an initial mechanical insult followed by a cascade of complex secondary reactions, with inflammation playing a central role (Tang et al., 2023; Vishwakarma et al., 2018). Post-SCI, the disruption of the blood-brain barrier and acute neuronal death lead to the release of numerous intracellular and extracellular molecules (Man Hoi and Yue, 2023). These molecules, acting as damage-associated molecular patterns (DAMPs), trigger local immune responses (Bortolotti et al., 2018). The initiation of inflammation involves multiple cell types, including microglia, astrocytes, and infiltrating peripheral immune cells (Okazaki et al., 2016). These cells collectively release a series of inflammatory mediators, such as TNF- α , IL-1 β , and IL-6. The expression of these cytokines rapidly increases following SCI, directly affecting neurons and glial cells, causing cell death and dysfunction (Mo et al., 2021). Additionally, they influence the polarization state of microglia, further amplifying the inflammatory response. Microglia, the intrinsic immune cells of the central nervous system, transition from a resting state to an activated state post-SCI, predominantly polarizing towards the M1 phenotype (Han et al., 2018; Liu et al., 2023). M1 microglia exhibit a pro-inflammatory profile, secreting large amounts of inflammatory cytokines, exacerbating local inflammation and neuronal damage (Lam et al., 2017). Over time, microglia can shift towards the M2 phenotype, which exhibits anti-inflammatory and reparative properties, secreting anti-inflammatory cytokines such as IL-10 and transforming growth factor- β (TGF- β), thereby promoting tissue repair and neuroregeneration (Ghosh et al., 2016). Current research highlights the importance of regulating microglial polarization and balancing the expression of pro-inflammatory and anti-inflammatory cytokines to mitigate secondary damage and promote functional recovery after SCI (Jiang et al., 2018; Liu et al., 2016).

I κ B α (Inhibitor of κ B α) is a critical inhibitor of the nuclear factor- κ B (NF- κ B), playing a significant role in the inflammatory response. NF- κ B is a family of transcription factors involved in regulating the expression of various inflammation-related genes. In a resting state, NF- κ B is bound to I κ B α in the cytoplasm, keeping it inactive (Colleran et al., 2011; Mamun et al., 2024). However, following SCI, injury signals activate the NF- κ B pathway through various mechanisms, leading to the phosphorylation and

degradation of I κ B α (Zhang et al., 2021). This process releases NF- κ B, allowing it to translocate to the nucleus and initiate the transcription of inflammation-related genes (Lv et al., 2021). The dysregulation of I κ B α is central to the inflammatory response post-SCI. Studies indicate that excessive degradation of I κ B α results in sustained activation of NF- κ B, which in turn leads to the overexpression of inflammatory mediators, exacerbating neuronal damage and inflammation. Thus, modulating the stability and function of I κ B α and balancing the activity of the NF- κ B pathway are crucial for mitigating secondary damage and promoting functional recovery after SCI. Current research suggests that pharmacological interventions or gene therapy targeting I κ B α expression and function could offer new therapeutic strategies for SCI.

In the inflammatory response following SCI, zinc ions play a multifaceted and crucial role. Zinc is not only an essential trace element in the central nervous system but also involved in a wide range of biological processes, including enzymatic catalysis, protein structure stabilization, and intracellular signal transduction (Wang et al., 2023). Extensive research has uncovered zinc intricate regulatory functions within cells, such as mitigating neuronal apoptosis by maintaining mitochondrial quality control, thereby protecting nerve cells from further damage (Bai et al., 2024). Additionally, zinc ions have shown potential in inhibiting certain inflammatory signaling pathways that could lead to pyroptosis post-SCI (Ye et al., 2022). Our research team has provided the first experimental evidence demonstrating that zinc ions alleviate the inflammatory response by upregulating I κ B α (Inhibitor of κ B α) expression. This finding is significant for understanding the mechanisms of zinc ions in SCI.

5 Conclusion

In summary, our comprehensive transcriptomic analysis has unveiled a novel mechanism of zinc ions in the treatment of spinal cord injury (SCI), particularly in regulating the inflammatory response. We discovered that zinc ions can reduce the production of inflammatory mediators and alleviate inflammation and cellular damage by upregulating I κ B α expression. Consistent validation results from in vitro experiments and mouse models of SCI demonstrate that zinc ions effectively mitigate the inflammatory response and cellular apoptosis post-SCI, offering new perspectives for SCI treatment. Our research not only elucidates the potential mechanisms of zinc ions in SCI therapy but also provides a theoretical foundation for developing new therapeutic strategies. Future studies could further explore the interactions of zinc ions with other signaling pathways and the specific regulatory mechanisms of zinc ions at different stages of SCI, offering more precise and effective treatment approaches and targets for SCI.

Data availability statement

The original contributions presented in the study are included in the article/Supplementary Material, further inquiries can be directed to the corresponding authors.

Ethics statement

The animal study was approved by Animal Protection Committee of Jinzhou Medical University. The study was conducted in accordance with the local legislation and institutional requirements.

Author contributions

DL: Conceptualization, Data curation, Investigation, Methodology, Validation, Writing—original draft, Writing—review and editing. MB: Formal Analysis, Methodology, Software, Visualization, Writing—original draft, Writing—review and editing. ZG: Data curation, Writing—review and editing. YC: Software, Validation, Writing—review and editing. XM: Funding acquisition, Project administration, Resources, Supervision, Writing—review and editing. HT: Funding acquisition, Project administration, Resources, Supervision, Writing—review and editing. ZS: Funding acquisition, Project administration, Resources, Supervision, Writing—review and editing.

Funding

The author(s) declare that financial support was received for the research, authorship, and/or publication of this article. This work was supported by grants from the National Natural Science Foundation of China (NO. 82272256) and Jinzhou Medical University Youth Science and Technology Talent Support Project (JYQT202204). Liaoning Provincial

References

- Bai, M., Cui, Y., Sang, Z., Gao, S., Zhao, H., and Mei, X. (2024). Zinc ions regulate mitochondrial quality control in neurons under oxidative stress and reduce PANoptosis in spinal cord injury models via the I κ B α -Bax pathway. *Free Radic. Biol. Med.* 221, 169–180. doi:10.1016/j.freeradbiomed.2024.05.037
- Bortolotti, P., Faure, E., and Kipnis, E. (2018). Inflammasomes in tissue damages and immune disorders after trauma. *Front. Immunol.* 9, 1900. doi:10.3389/fimmu.2018.01900
- Brennan, F. H., Li, Y., Wang, C., Ma, A., Guo, Q., Li, Y., et al. (2022). Microglia coordinate cellular interactions during spinal cord repair in mice. *Nat. Commun.* 13, 4096. doi:10.1038/s41467-022-31797-0
- Caffarel, M. M., and Braza, M. S. (2022). Microglia and metastases to the central nervous system: victim, ravager, or something else? *J. Exp. and Clin. Cancer Res.* 41, 327. doi:10.1186/s13046-022-02535-7
- Colleran, A., Ryan, A., O’Gorman, A., Mureau, C., Liptrot, C., Dockery, P., et al. (2011). Autophagosomal I κ B α degradation plays a role in the long term control of tumor necrosis factor- α -induced nuclear factor- κ B (NF- κ B) activity. *J. Biol. Chem.* 286, 22886–22893. doi:10.1074/jbc.m110.199950
- Deng, H., Liu, Y., Shi, Z., Yang, J., Liu, C., and Mei, X. (2023). Zinc regulates a specific subpopulation of VEGFA + microglia to improve the hypoxic microenvironment for functional recovery after spinal cord injury. *Int. Immunopharmacol.* 125, 111092. doi:10.1016/j.intimp.2023.111092
- Fan, H., Tang, H.-B., Chen, Z., Wang, H.-Q., Zhang, L., Jiang, Y., et al. (2020). Inhibiting HMGB1-RAGE axis prevents pro-inflammatory macrophages/microglia polarization and affords neuroprotection after spinal cord injury. *J. Neuroinflammation* 17, 295. doi:10.1186/s12974-020-01973-4
- Ge, M. h., Tian, H., Mao, L., Li, D. y., Lin, J. q., Hu, H. s., et al. (2021). Zinc attenuates ferroptosis and promotes functional recovery in contusion spinal cord injury by activating Nrf2/GPX4 defense pathway. *CNS Neurosci. and Ther.* 27, 1023–1040. doi:10.1111/cns.13657
- Ghosh, M., Xu, Y., and Pearce, D. D. (2016). Cyclic AMP is a key regulator of M1 to M2a phenotypic conversion of microglia in the presence of Th2 cytokines. *J. Neuroinflammation* 13, 9. doi:10.1186/s12974-015-0463-9
- Groeger, A. L., Cipollina, C., Cole, M. P., Woodcock, S. R., Bonacci, G., Rudolph, T. K., et al. (2010). Cyclooxygenase-2 generates anti-inflammatory mediators from omega-3 fatty acids. *Nat. Chem. Biol.* 6, 433–441. doi:10.1038/nchembio.367
- Han, D., Yu, Z., Liu, W., Yin, D., Pu, Y., Feng, J., et al. (2018). Plasma Hemopexin ameliorates murine spinal cord injury by switching microglia from the M1 state to the M2 state. *Cell Death and Dis.* 9, 181. doi:10.1038/s41419-017-0236-8
- Huang, Z., Wang, J., Li, C., Zheng, W., He, J., Wu, Z., et al. (2022). Application of natural antioxidants from traditional Chinese medicine in the treatment of spinal cord injury. *Front. Pharmacol.* 13, 976757. doi:10.3389/fphar.2022.976757
- Iaffaldano, P., Lucisano, G., Caputo, F., Paolicelli, D., Patti, F., Zaffaroni, M., et al. (2021). Long-term disability trajectories in relapsing multiple sclerosis patients treated with early intensive or escalation treatment strategies. *Ther. Adv. Neurological Disord.* 14, 17562864211019574. doi:10.1177/17562864211019574
- Irrera, N., Vaccaro, M., Bitto, A., Pallio, G., Pizzino, G., Lentini, M., et al. (2017). BAY 11-7082 inhibits the NF- κ B and NLRP3 inflammasome pathways and protects against IMQ-induced psoriasis. *Clin. Sci. (Lond)* 131, 487–498. doi:10.1042/CS20160645
- Jiang, D., Yang, X., Ge, M., Hu, H., Xu, C., Wen, S., et al. (2023). Zinc defends against Parthanatos and promotes functional recovery after spinal cord injury through SIRT3-mediated anti-oxidative stress and mitophagy. *CNS Neurosci. and Ther.* 29, 2857–2872. doi:10.1111/cns.14222
- Jiang, M., Liu, X., Zhang, D., Wang, Y., Hu, X., Xu, F., et al. (2018). Celastrol treatment protects against acute ischemic stroke-induced brain injury by promoting an IL-33/ST2 axis-mediated microglia/macrophage M2 polarization. *J. Neuroinflammation* 15, 78. doi:10.1186/s12974-018-1124-6
- Lam, D., Lively, S., and Schlichter, L. C. (2017). Responses of rat and mouse primary microglia to pro- and anti-inflammatory stimuli: molecular profiles, K⁺ channels and migration. *J. Neuroinflammation* 14, 166. doi:10.1186/s12974-017-0941-3
- Li, D., Tian, H., Li, X., Mao, L., Zhao, X., Lin, J., et al. (2020). Zinc promotes functional recovery after spinal cord injury by activating Nrf2/HO-1 defense pathway and

Science and Technology Program Project Number: 2022-MS-457.

Conflict of interest

The authors declare that the research was conducted in the absence of any commercial or financial relationships that could be construed as a potential conflict of interest.

Generative AI statement

The author(s) declare that no Generative AI was used in the creation of this manuscript.

Publisher’s note

All claims expressed in this article are solely those of the authors and do not necessarily represent those of their affiliated organizations, or those of the publisher, the editors and the reviewers. Any product that may be evaluated in this article, or claim that may be made by its manufacturer, is not guaranteed or endorsed by the publisher.

Supplementary material

The Supplementary Material for this article can be found online at: <https://www.frontiersin.org/articles/10.3389/fphar.2025.1510372/full#supplementary-material>

- inhibiting inflammation of NLRP3 in nerve cells. *Life Sci.* 245, 117351. doi:10.1016/j.lfs.2020.117351
- Liu, W., Rong, Y., Wang, J., Zhou, Z., Ge, X., Ji, C., et al. (2020). Exosome-shuttled miR-216a-5p from hypoxic preconditioned mesenchymal stem cells repair traumatic spinal cord injury by shifting microglial M1/M2 polarization. *J. Neuroinflammation* 17, 47. doi:10.1186/s12974-020-1726-7
- Liu, X., Berry, C. T., Ruthel, G., Madara, J. J., MacGillivray, K., Gray, C. M., et al. (2016). T cell receptor-induced nuclear factor κ B (NF- κ B) signaling and transcriptional activation are regulated by STIM1- and orai1-mediated calcium entry. *J. Biol. Chem.* 291, 8440–8452. doi:10.1074/jbc.M115.713008
- Liu, X., Tang, M., He, T.-Y., Zhao, S., Li, H.-Z., Li, Z., et al. (2023). Resveratrol improves paclitaxel-induced cognitive impairment in mice by activating SIRT1/PGC-1 α pathway to regulate neuronal state and microglia cell polarization. *Drug Des. Dev. Ther.* 17, 1125–1138. doi:10.2147/DDDT.S400936
- Lv, C.-L., Gao, K., Zhang, T., Li, K., and Zhang, Z.-L. (2021). LncRNA Airsci increases the inflammatory response after spinal cord injury in rats through the nuclear factor kappa B signaling pathway. *Neural Regen. Res.* 16, 772–777. doi:10.4103/1673-5374.295335
- Mamun, A. A., Shao, C., Geng, P., Wang, S., and Xiao, J. (2024). Polyphenols targeting NF- κ B pathway in neurological disorders: what we know so far? *Int. J. Biol. Sci.* 20, 1332–1355. doi:10.7150/ijbs.90982
- Man Hoi, M., and Yue, Q. (2023). Emerging roles of astrocytes in blood-brain barrier disruption upon amyloid-beta insults in Alzheimer's disease. *Neural Regen. Res.* 0, 0. doi:10.4103/1673-5374.367832
- Mizobuchi, H., and Soma, G.-I. (2021). Low-dose lipopolysaccharide as an immune regulator for homeostasis maintenance in the central nervous system through transformation to neuroprotective microglia. *Neural Regen. Res.* 16, 1928–1934. doi:10.4103/1673-5374.308067
- Mo, X., Liu, M., Gong, J., Mei, Y., Chen, H., Mo, H., et al. (2022). PTPRM is critical for synapse formation regulated by zinc ion. *Front. Mol. Neurosci.* 15, 822458. doi:10.3389/fnmol.2022.822458
- Mo, Z.-T., Zheng, J., and Liao, Y.-I. (2021). Icaritin inhibits the expression of IL-1 β , IL-6 and TNF- α induced by OGD/R through the IRE1/XBP1s pathway in microglia. *Pharm. Biol.* 59, 1473–1479. doi:10.1080/13880209.2021.1991959
- Muñoz García, A., Juksar, J., Groen, N., Zaldumbide, A., de Koning, E., and Carlotti, F. (2024). Single-cell transcriptomics reveals a role for pancreatic duct cells as potential mediators of inflammation in diabetes mellitus. *Front. Immunol.* 15, 1381319. doi:10.3389/fimmu.2024.1381319
- Okazaki, R., Doi, T., Hayakawa, K., Morioka, K., Imamura, O., Takishima, K., et al. (2016). The crucial role of Erk2 in demyelinating inflammation in the central nervous system. *J. Neuroinflammation* 13, 235. doi:10.1186/s12974-016-0690-8
- Pajarillo, E., Nyarko-Danquah, I., Digman, A., Vied, C., Son, D. S., Lee, J., et al. (2022). Astrocytic Yin Yang 1 is critical for murine brain development and protection against apoptosis, oxidative stress, and inflammation. *Glia* 71, 450–466. doi:10.1002/glia.24286
- Sang, Z., Liang, Z., Xuelian Huang, G., Chen, Z., Ren, X., and Mei, X. (2024). NIR sensitive ZnO QDs decorated MXene hydrogel promotes spinal cord repair via tunable controlled release of Zn²⁺ and regulating ROS microenvironment of mitochondrion. *Chem. Eng. J.* 489, 151343. doi:10.1016/j.cej.2024.151343
- Sun, Y.-X., Xu, A.-H., Yang, Y., Shao, Y., and Jiang, M.-Y. (2022). Different frequencies of repetitive transcranial magnetic stimulation combined with local injection of botulinum toxin type A for post-stroke lower limb spasticity: study protocol for a prospective, single-center, non-randomized, controlled clinical trial. *Neural Regen. Res.* 17, 2491–2496. doi:10.4103/1673-5374.339011
- Tan, K., Zhu, H., Zhang, J., Ouyang, W., Tang, J., Zhang, Y., et al. (2019). CD73 expression on mesenchymal stem cells dictates the reparative properties via its anti-inflammatory activity. *Stem Cells Int.* 2019, 1–12. doi:10.1155/2019/8717694
- Tang, H., Gu, Y., Jiang, L., Zheng, G., Pan, Z., and Jiang, X. (2023). The role of immune cells and associated immunological factors in the immune response to spinal cord injury. *Front. Immunol.* 13, 1070540. doi:10.3389/fimmu.2022.1070540
- Van Broeckhoven, J., Erens, C., Sommer, D., Scheijen, E., Sanchez, S., Vidal, P. M., et al. (2022). Macrophage-based delivery of interleukin-13 improves functional and histopathological outcomes following spinal cord injury. *J. Neuroinflammation* 19, 102. doi:10.1186/s12974-022-02458-2
- Vishwakarma, S. K., Bardia, A., Lakkireddy, C., Paspala, S. A. B., and Khan, A. A. (2018). Bioengineering human neurological constructs using decellularized meningeal scaffolds for application in spinal cord injury. *Front. Bioeng. Biotechnol.* 6, 150. doi:10.3389/fbioe.2018.00150
- Wang, Y., Huang, N., and Yang, Z. (2023). Revealing the role of zinc ions in atherosclerosis therapy via an engineered three-dimensional pathological model. *Adv. Sci.* 10, e2300475. doi:10.1002/advs.202300475
- Xu, C., Zhou, Z., Zhao, H., Lin, S., Zhang, P., Tian, H., et al. (2023). Zinc promotes spinal cord injury recovery by blocking the activation of NLRP3 inflammasome through SIRT3-mediated autophagy. *Neurochem. Res.* 48, 435–446. doi:10.1007/s11064-022-03762-2
- Ye, C., Lian, G., Wang, T., Chen, A., Chen, W., Gong, J., et al. (2022). The zinc transporter ZIP12 regulates monocrotaline-induced proliferation and migration of pulmonary arterial smooth muscle cells via the AKT/ERK signaling pathways. *BMC Pulm. Med.* 22, 111. doi:10.1186/s12890-022-01905-3
- Zhang, G. Z., Liu, M. Q., Chen, H. W., Wu, Z. L., Gao, Y. C., Ma, Z. J., et al. (2021). NF- κ B signalling pathways in nucleus pulposus cell function and intervertebral disc degeneration. *Cell Prolif.* 54, e13057. doi:10.1111/cpr.13057
- Zhao, S., Xiao, P., Cui, H., Gong, P., Lin, C., Chen, F., et al. (2020). Hypothermia-induced ubiquitination of voltage-dependent anion channel 3 protects BV2 microglia cells from cytotoxicity following oxygen-glucose deprivation/recovery. *Front. Mol. Neurosci.* 13, 100. doi:10.3389/fnmol.2020.00100